Towards an automated masking process – a model-based approach

Journal:	*Part B: Journal of Engineering Manufacture*
Manuscript ID	JEM-17-0025.R3
Manuscript Type:	Original article
Date Submitted by the Author:	n/a
Complete List of Authors:	Elgeneidy, Khaled; Loughborough University, Wolfson School of Mechanical, Electrical and Manufacturing Engineering Al-Yacoub, Ali; Loughborough University, Intelligent Automation Usman, Zahid ; Coventry Univesrity, Institute for Advanced Manufacturing and Engineering Lohse, Niels; University of Nottingham, Jackson, Michael; University of Loughborough, Wright, Iain; Rolls-Royce, Automation Systems
Keywords:	Masking, Control, Modelling, Automation, Time-pressure dispensing, Manufacturing, aerospace
Abstract:	The masking of aircraft engine parts, such as turbine blades, is a major bottleneck for the aerospace industry. The process is often carried out manually in multiple stages of coating and curing, which requires extensive time and introduces variations in the masking quality. This paper investigates the automation of the masking process utilising the well-established time-pressure (T/P) dispensing process for controlled maskant dispensing, and a robotic manipulator for accurate part handling. A mathematical model for the T/P dispensing process was derived, extending previous models from the literature by incorporating the robot velocity for controlled masking line width. An experiment was designed, based on the theoretical analysis of the dispensing process, to derive an empirical model from the generated data that incorporates the losses that are otherwise difficult to model mathematically. The model was validated under new input conditions to demonstrate the feasibility of the proposed approach and the masking accuracy using the derived model.

Towards an automated masking process – a model-based approach

Khaled Elgeneidy[1], Ali Al-Yacoub[1], Zahid Usman[2], Niels Lohse[1], Michael Jackson[1], Iain Wright[3].

Corresponding author:

Khaled Elgeneidy, EPSRC centre for Intelligent Automation, Loughborough University, Epinal Way, Loughborough, UK.

Email: mmkame@lboro.ac.uk

Keywords

Masking, Control, Modelling, Automation, Time-pressure dispensing, Manufacturing.

Abstract

The masking of aircraft engine parts, such as turbine blades, is a major bottleneck for the aerospace industry. The process is often carried out manually in multiple stages of coating and curing, which requires extensive time and introduces variations in the masking quality. This paper investigates the automation of the masking process utilising the well-established time-pressure (T/P) dispensing process for controlled maskant dispensing, and a robotic manipulator for accurate part handling. A mathematical model for the T/P dispensing process was derived, extending previous models from the literature by incorporating the robot velocity for controlled masking line width. An experiment was designed, based on the theoretical analysis of the dispensing process, to derive an empirical model from the generated data that incorporates the losses that are otherwise difficult to model mathematically. The model was validated under new input conditions

[1] EPSRC centre for Intelligent Automation, Loughborough University, Loughborough, UK.
[2] Coventry University, Institute for Advanced Manufacturing and Engineering, Coventry, UK.
[3] Rolls-Royce, Automation Systems, Derby, UK.

to demonstrate the feasibility of the proposed approach and the masking accuracy using the derived model.

1 Introduction:

Many high-performance engineering components require localised surface treatments to improve their heat resistance, surface hardness, friction, and other mechanical properties[1]. Most of these processes are difficult to apply locally and require those areas which do not need to be treated to be protected. Therefore, different masking processes are needed to ensure that the surface treatment is only applied to the desired areas. The application of the maskant, commonly in liquid form, is often a labour-intensive process which requires skilled workers who use their experience and senses to manually mask each part within the specified tolerances [2]. This process typically requires several cycles, where in each cycle a layer of maskant is applied and cured until a required thickness has been achieved. Although skilled operators can mask the parts within the defined tolerances, the manual process is tedious and time-consuming due to the repetitive cycles of coating and curing [3]. In addition, valuable time and money are spent on training the operators to acquire the relevant skills for accurate masking [4].

Moreover, the automation of other processes involving dispensing of viscous liquids similar to the masking process has been previously investigated such as: robotic sealing of aerospace parts [5], robotic coating for space solar modules [6], robotic spray painting for automotive parts [7,8], robotic workstations for small volume liquid dispensing and handling in laboratories [9]. In addition, automation of different processes in the aircraft manufacturing and assembly is being increasingly sought after [10,11]. However, limited attention has been directed towards automating the manual masking operations, despite being a significant bottleneck for repetitive production processes involving components with complex geometries, such as the case for turbine blades in aircraft engines [12]. Manual masking introduces variations in both the resulting mask quality as well as the curing time [3]. This highlights the need to make the masking process faster and more consistent, which can be achieved through automation. However, this involves a number of challenges that need to be considered including: i) the modelling and control of the

masking process, ii) adaptability in masking according to the areas to be masked, iii) automated path planning, and iv) ensuring acceptable masking quality.

This paper investigates an automated masking system in which the target object is handled using a robotic arm, while the maskant material is dispensed using the well-established time-pressure dispensing system. At present, several models exist for the fluid dispensing using time-pressure systems that could be associated with masking operations. However, since the time-pressure dispensing system typically involves a stationary target object, the influence of the robotic manipulator used in the proposed system here needs to be incorporated into the model to control the masking process. Thus, the main contribution of this paper is in deriving a model that is used to control the automatic application of the maskant material on different target areas, by tuning the velocity of the robot holding the target object according to the input process parameters. The emphasis of this research has been on the ability to automatically mask a specific area of a planar part with a homogeneous maskant layer in a single attempt, without the need for repetitive stages of coating and curing. This has the potential of not only reducing the duration of the masking process, but also helping in achieving consistent masking quality.

The paper is organised as follows. Section 2 presents a review of the previous work in modelling of dispensing systems that -can be utilised for the masking process. The following section presents the mathematical modelling of the time-pressure dispensing process, starting from a dynamic model and simplifying this to a steady state model under a given assumption. This is then followed by the empirical modelling of the system through design of experiments, based on the outcomes of the theoretical modelling. The proposed masking system using the developed empirical model is then tested and the results reported in section 4. Finally, the papers conclude with considering the initial feasibility of the proposed system and discussion of future research work.

2 Previous Work

An inspiration for automated masking comes from the additive manufacturing processes and robotic painting or spraying. However, additive manufacturing of parts that are printed from scratch is not suitable to adopt for automated masking, since dispensing

does not occur on top of an existing component and the materials used are much simpler in their flow behaviour than masking materials [13–15]. Yet, the more advanced robotic additive manufacturing where additive manufacturing is performed over free-form surfaces and complex geometries are more relevant [16]. However, the material properties and flow are significantly different from the case of masking, as the dispensed material takes the required form almost immediately. Whereas, masking is mostly performed using vicious liquid materials that require long curing times. Moreover, several approaches are currently being used for masking of aerospace, automotive and electronic components, such as dipping, spraying and dispensing. Dipping and spraying approaches are mostly used for parts with simple geometric features and are difficult to employ for masking specific areas on parts with complex geometries [17].The dispensing approach, however, can be used for masking complex shapes and is widely used in industries for applications such as advanced integrated circuits encapsulation (AICE) and surface mount technology (SMT) [18]. In general, dispensing mechanisms can be classified into contact based and non-contact based mechanisms, such as volumetric dispensing and jetting respectively [18]. One of the most commonly used dispensing mechanisms is the Time/Pressure (T/P) dispensing due to its simplicity, low cost, and ease of operation and maintenance [19].

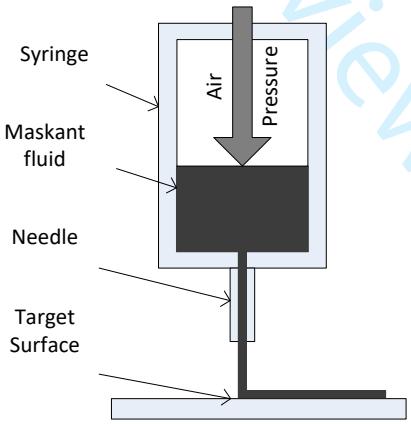

Figure 1: Schematic diagram of a typical T/P dispensing process

In T/P dispensing, an electrical solenoid controls the pressurised air in the syringe for pushing the fluid out of the needle onto the workpiece as illustrated in Figure 1. Controlling the T/P dispensing requires knowledge about several variables that govern the process such as; pressure in the syringe, needle diameter, distance from the part, and

fluid properties [20]. Different mathematical models have been previously proposed for covering various aspects of the T/P dispensing process [20–22]. The behaviour of T/P process can be modelled as a dynamic system or as a steady state system. The dynamic behaviour models of T/P system under both Newtonian (constant viscosity) and Non-Newtonian fluids (varying viscosity) have been presented in [23–26]. Although a simplified dynamic model based on simple physical relations was presented and experimentally verified [18], dynamic models still involve a large number of variables which can be difficult to control. For this reason, many researchers have modelled the T/P system as a steady state system to simplify the model with acceptable accuracy [27]. These models assume that the dispensed fluid has a constant viscosity and that the inconsistency in the flow at the start and the end of the masking process is negligible [18]. Models of the T/P dispensing system currently do not incorporate the relative movement between the dispensing system and a robotic manipulator handling the target part. In addition, these models have been developed explicitly for point and line dispensing applications only. However, many automotive and aircraft components require masking over an area, which so far has not been investigated in detail by the research community using T/P dispensing. In this context, there is a need to explore the effect of the robot's velocity on the T/P dispensing process and resulting area coverage. This paper investigates a model of the masking process for area coverage using T/P dispensing that incorporates the relative velocity between a manipulator and the dispenser. The principal objective is to better control the area coverage in automated masking applications.

3 Modelling of Automated Masking

Figure 2 shows schematics for the masking process using a T/P dispensing system that is automated using a robotic manipulator controlling the movement of the target object under the needle of the dispensing system. The model for the robotic masking system was developed in two main stages. In the first stage, a mathematical model for the system was developed, which extends the dispensing model form [28] by incorporating the velocity of the robotic manipulator. This allowed identifying the key variables that should be included when designing an experiment for deriving an empirical model for the automated masking process. In the second stage, the empirical model was derived, based

on the identified key parameters, using experimental data generated from running a series of robotic masking operations. Finally, the derived model was deployed to the robot controller to control the masking process and validate the overall approach.

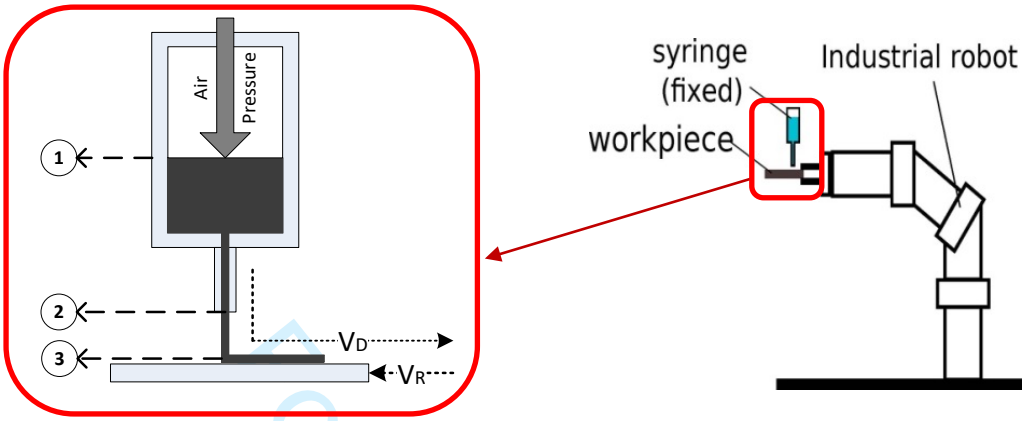

Where:

- V_D: Dispensing fluid velocity
- V_R: Relative robot/surface velocity

Figure 2: Schematic diagrams of the time pressure dispensing process as part of an automated dispensing setup

3.1 Mathematical Modelling

There are many variables which affect the T/P dispensing system, most of which can be controlled depending on the hardware setup. Nevertheless, there are some variables which are highly dynamic especially when dispensing a large amount during a masking process. The most significant dynamic variables that affect the consistency of the dispensed fluid include the chamber volume, the dispensing fluid volume, and the air pressure in the syringe chamber. Most dynamic models focus on representing only the most influential variables to contain the complexity of the model. For the model used in this paper, it is assumed that the fluid properties such as its compressibility and viscosity are constant over time and that there is dry friction between the syringe and the fluid. Additionally, the delay that could be caused by the pneumatic lines was ignored. Hence, the simplified dynamic model proposed in [28] for these specific assumptions was adopted. This model is presented in equation (1) where S is the Laplace operator, K is viscosity coefficient, 'L_n' is needle length, 'D_n' is needle diameter, 'ρ' is maskant fluid density, 'ΔP' is dispensing pressure inside the syringe, and 'V_d' is the dispensing fluid velocity.

$$\frac{V_d(s)}{\Delta P} = \frac{32K\frac{L_n}{{D_n}^2}}{\frac{\rho {D_n}^2}{32KL_n}S+1} = \frac{K_0}{K_1 S+1} \qquad (1)$$

The relative velocity between the dispensed fluid and the robot end effector (illustrated in Figure 2) can be defined as in Equation (2). Hence, substituting equation (1) into (2) results in equation (3), which defines the relative velocity 'V_r' between the robot velocity 'V_R' and the dispensing fluid velocity 'V_d'. The mathematical model shows the dynamical behaviour properties which is a typical first order system as shown in Equation (3).

$$V_r(s) = V_R - V_d(s) \qquad (2)$$

$$V_r(s) = V_R - \frac{K_0 \times \Delta P}{K_1 S+1} \qquad (3)$$

In general, the T/P system has a time delay of around 50~200 mS because of the long transmission pipe, pressure variation in syringe chamber, distance between the tip of the needle and the surface of the workspace and fluid resistance [29]. Figure 3 depicts the step response of the system defined in Equation (3). The response shows a delay of ~86 mS, without considering the possible delay from the transmission lines. Such delay would influence the consistency of the dispensed maskant at the start and end of the operation until the processes reach a steady state.

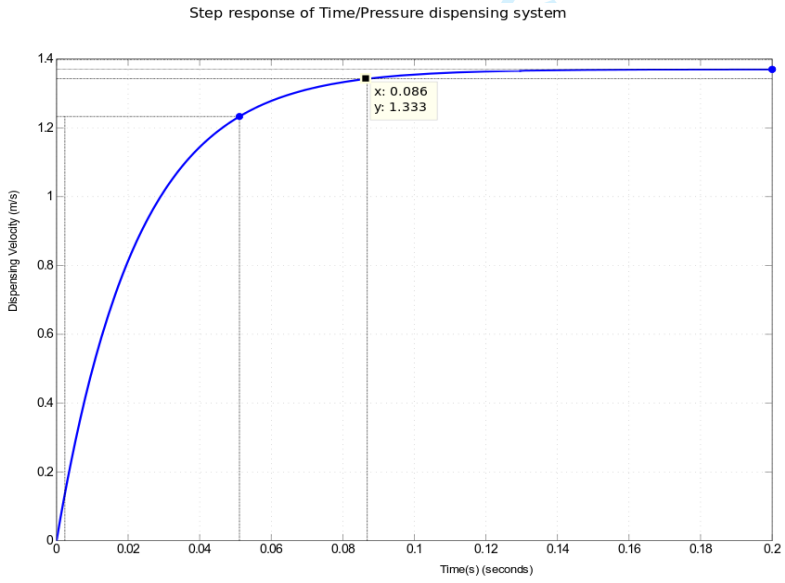

Figure 3: Time/Pressure step response of the dynamic system defined in Equation (3)

To overcome the delay problem, a time delay function can be used at the start and end points of the dispensing process to eliminate missing and excessive maskant at the beginning and end of the process respectively. A waiting function is a simple solution which is particularly suitable for short to medium dispensing periods since the variation in the syringe chamber pressure can be neglected. However, for long dispensing runs where the pressure in the syringe changes significantly, more sophisticated solutions will be required. For continuous short run dispensing applications considered here, the transition delay at the start and end points, as well as the variation of the dispensing parameter during operating time can be neglected. Therefore, the system behaviour can be modelled as a steady state model, which simplifies Equation (3) as follows:

$$V_r(s) = V_R - K_0 \times \Delta P$$

By considering the cross-sectional geometry of a single dispensed line, the covered area can be determined using the empirical approximation in Equation (4), relating the width 'W' and length 'L' of the dispensed maskant line

$$\begin{aligned} A_c(t) = &\quad W(t) * L(t) \\ \approx &\quad 1.45 * D_n * L(t) \end{aligned} \qquad (4)$$

By substituting Equation (4) into the Equation (3) and applying the continuity equation, a relation will result between the dispensed line width (output) and the robot speed (input) as shown in Equation (5)

$$\ln(W(t)) \approx \frac{1}{2}\left(\ln(32KL_n) + 4\ln(D_n) + \ln(\Delta P) - \ln\left(32K\frac{L_n}{{D_n}^2} * \Delta P - V_R\right)\right) \qquad (5)$$

Equation (5) shows the mathematical relation that maps the robot velocity to the dispensed line width. It neglects the time delay caused by the dynamical elements in the system. As a result, the dispensing problem can now be viewed as a steady state fluid flow problem. In this case, Equation (6) for the dispensing fluid velocity 'V_d' exiting the needle can be derived using Bernoulli's equation between points 1 and 2 labelled on Figure 2. Where, 'L_f' is the length of the fluid inside the syringe and '$\sum F$' is the combined frictional losses inside the needle.

$$V_d = \sqrt{\left[\frac{(\Delta P)}{\rho} + g\left(L_n + L_f\right) - \sum F\right]} \qquad (6)$$

When the robotic manipulator controlling the displacement of the target object under a stationary dispensing needle, the relative velocity between the needle and the moving object will be equivalent to the controlled robot velocity robot 'V_R'. Hence, by programming the planar movement of the robot underneath the needle, lines of the masking material can be dispensed on the object with a cross-sectional area 'A_{Line}'. According to the continuity theory, the fluid flow rate leaving a needle of diameter 'D_n' at point 2 is equivalent to the flow rate of the material dispensed on the moving plate at point 3 (Figure 2). This leads to the following relation:

$$\frac{\pi}{4}{D_n}^2 \times V_d = A_{line} \times V_R \qquad (7)$$

By substituting Equation (6) for the fluid dispensing velocity into Equation (7), the cross-sectional area of the dispensed maskant line on the plate can be defined as:

$$A_{line} = \frac{\frac{\pi}{4}{D_n}^2\sqrt{\left[\frac{\Delta P}{\rho}+g(L_n+L_f)-\sum F\right]}}{V_R} \qquad (8)$$

Applying a natural log function to linearise the equation results in the following final equation describing the cross-sectional area of a dispensed maskant line that accommodates the robot velocity, where 'F' is a coefficient representing the combined the frictional loses:

$$ln(A_{line}) = \frac{\pi}{2}ln(D_n) - ln(V_R) + \frac{1}{2}ln(\Delta P + F\rho) - \frac{1}{2}ln\,\rho \qquad (9)$$

This mathematical model provides an understanding of the main parameters controlling the outcome of the T/P dispensing process. This can be used as a good starting point to guide the development of a simple empirical model that captures the unknown losses in the system that are difficult to accurately model mathematically and is influenced by the hardware used in the system. The model thus shows that the cross-sectional area of the maskant lines dispensed from a stationary needle on a moving target object is a function of three primary variables, which are (i) the needle diameter D_n, (ii) the end effector velocity of the robot V_R, and (iii) the applied dispensing pressure ΔP. While, the effects of the frictional losses with the needle walls and the pressure drop inside the syringe are incorporated within the unknown coefficient 'F'. Hence, this mathematical model has helped to identify the key parameters required for modelling the system. An empirical

model for the time-pressure system will be derived that considers those parameters identified through the derivation of the mathematical model, while implicitly accounting for the unknown frictional coefficient.

3.2 Empirical Modelling

Following the identification of the key process variables, a set of experiments were conducted to derive an empirical model that predicts the dimensions of the dispensed masking lines resulting from the time-pressure dispensing process, while incorporating the unknown frictional losses that are otherwise difficult to model mathematically. Through systematic experimentation, the unknown model coefficients can be empirically approximated from experimental data captured from the actual masking process and fed to a statistical analysis software to conduct an analysis of variance and regression. The resulting empirical model can then be easily integrated within the robot controller for the offline control of the masking process.

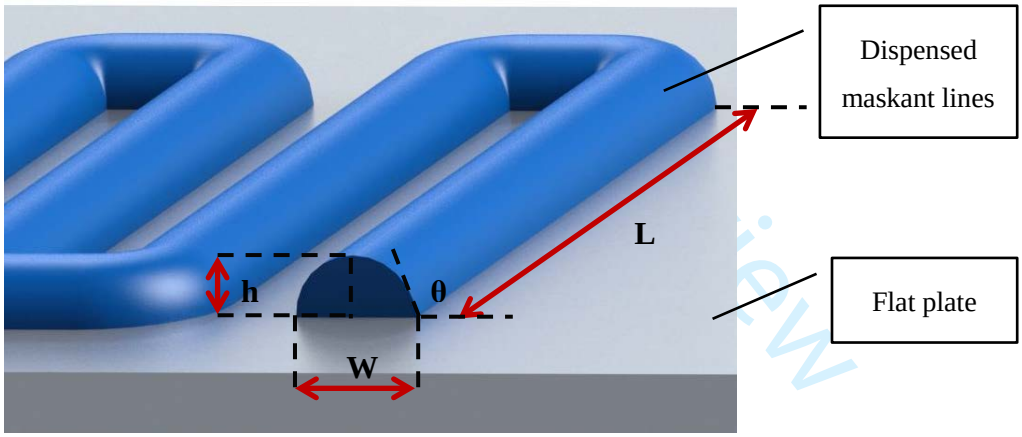

Figure 4: Illustration showing the geometry and dimensions of maskant lines dispensed on a flat surface

The geometric variables defining the typical geometry and cross-sectional area of maskant lines dispensed in a raster pattern on a flat surface are illustrated in Figure 4. The main parameter of interest here is the width '*W*' of the dispensed maskant lines, since being able to predict its value can be used to determine the required spacing between the maskant lines that would result in a homogenously masked area with no gaps or excessive overlaps. The length of the maskant lines is directly controllable through the programmed movement of the robotic manipulator holding the target object and hence

does not need to be studied in the experiment. While the height of the maskant lines can be mathematically estimated based on the wetting coefficient and surface tension [28], and is generally not a significantly critical factor for many masking applications as long as the target area is well covered. Therefore, the output parameter that needs to be investigated in the designed experiment is only the width of maskant lines, which can be measured via 2D image processing. On the other hand, the input process parameters of interested are the ones identified in the mathematical model. Hence, the aim of the experiment is to derive an empirical relation between the V_R, ΔP, and D_n process parameters and the process response W, assuming any other nuisance factors can be either held constant or have a negligible effect the studied response.

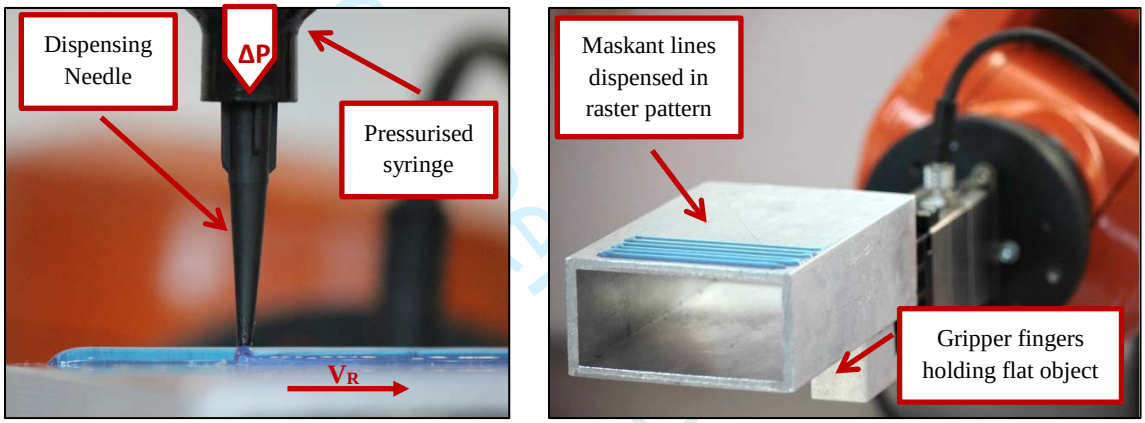

Figure 5: Components of the automated masking setup

The experimental setup is shown in Figure 5, featuring an ABB IRB120 robotic arm with a two-fingered gripper grasping a flat object from a fixed reference, as well as a controlled pressure dispensing unit (Fisnar JB1113N) pressurising the syringe containing the maskant material that flows through a UV shielded needle. In order to ensure that the initial assumptions made during the mathematically modelling of the process as a steady state system are justified, a number of practical considerations were implemented. Firstly (i), a long needle length of 12 mm was used to guarantee a fully developed fluid flow as it reaches the tip of the needle. Secondly (ii), a large syringe to needle diameter ratio was used to ensure that the fluid velocity inside the syringe was relatively small. Thirdly (iii), the masking material (DYM 728-G) was used which can be treated as an incompressible

Newtonian fluid, as confirmed by the constant viscosity given by the material specification[4].

The robot was programmed to move the object with the desired velocity beneath the stationary dispensing needle, so as to create a raster pattern of five equally spaced lines. A spacing distance of 5 mm was maintained to ensure that there will always be a clear gap between the lines, to enable a 2D image processing program to recognise each line and measure its width separately. This achieved by imaging the masked samples at the end of each run using a fixed camera setup and feeding those images to the developed image processing on MATLAB. The program uses standard thresholding and segmentation algorithms to isolate the blobs representing the dispensed lines from the background and makes the required width measurements after calibration, as shown in Figure 6. This provides a reliable non-contact measurement technique with a consistent accuracy, which was evaluated by measuring the spacing distance between the lines for each run and comparing this to its known value of 5 mm. The spacing measurements throughout the experiment were found to have an average error of only 0.02 mm and a standard deviation of 0.048, confirming the measurement accuracy for this imaging technique.

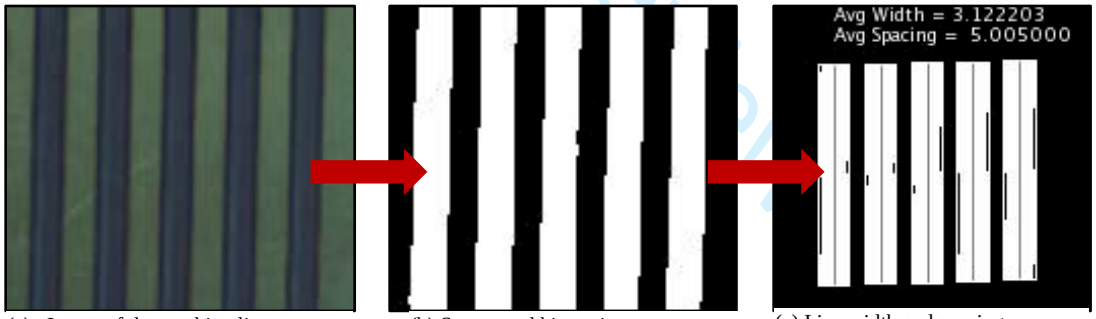

(a) Image of the masking lines on a flat plate
Actual Line Width: 3.10mm
Actual Spacing: 5mm

(b) Segmented binary image identifying the maskant lines.
Note: Broken lines are due to default display resolution

(c) Line width and spacing measured through the vision system
Mean width = 3.12 mm
Mean spacing = 5.005 mm

Figure 6: Vision system identifying the dispensed lines and measuring their average width

A multi-level factorial design model was used in designing the experiment by studying the three input parameters at different levels, against the measured response W. The

[4] https://www.dymax.com/images/pdf/pds/728-g.pdf

values of the levels for each parameter were chosen to cover the expected operating range so that the model can effectively capture the variance in the process. The V_R parameter was tested at values of 20, 30, and 40 mm, which is directly set using the robot controller. While the ΔP was tested at values of 10, 16, and 20 Psi, which is set using the analogue gauge of a pressure controlled dispensing unit. As for the D_n parameter, two needle sizes of 1.2 and 1.6 mm were tested in this experiment. Table 1 summarises the implemented experimental runs that covered all the combinations between the different factor levels. For each run, the recorded width value is the average width of the dispensed five lines.

Table 1: Experimental data from of the verification tests

#	Run	Factors			Response
		V_R	ΔP	D_n	W
		mm/s	Psi	mm	mm
1	15	20	10	1.2	1.93
2	7	30	10	1.2	1.56
3	3	40	10	1.2	1.50
4	9	20	16	1.2	2.34
5	12	30	16	1.2	2.02
6	2	40	16	1.2	1.94
7	17	20	20	1.2	2.48
8	18	30	20	1.2	2.08
9	13	40	20	1.2	1.96
10	16	20	10	1.6	2.51
11	1	30	10	1.6	1.96
12	5	40	10	1.6	1.73
13	4	20	16	1.6	2.73
14	11	30	16	1.6	2.51
15	10	40	16	1.6	2.45
16	6	20	20	1.6	3.53
17	14	30	20	1.6	2.91
18	8	40	20	1.6	2.65

3.2.1 Results and Discussion

Afterwards, the resulting set of experimental data was fed into a statistical analysis software (Design Expert) to evaluate the data using analysis of variance and derive the empirical model using regression analysis. Applying a natural log transformation to the

experimental data was found to linearise the data and result in an improved model fit. The resulting empirical model relating the studied process parameters to the measured response is presented in Equation (10). It can be noticed that the equation follows the same structure as the mathematical model derived earlier in Equation (9). This confirms the conceptual validity of the derived model. Yet for the empirical model, the unknown coefficients and losses that were difficult to calculate mathematically can be approximated and implicitly captured within the model based on data from actual runs.

$$\boldsymbol{ln(W)} = 0.860 * \boldsymbol{ln(D)} - 0.352 * \boldsymbol{ln(V)} + 0.477 * \boldsymbol{ln(P)} - 7.205 \quad (10)$$

The values of widths predicted by the empirical model were plotted against the actual widths from the conducted experiments (Figure 7) to evaluate the accuracy of the model. It can be observed that the points follow an almost linear relationship with an R^2 value of 0.947, mean error of 0.098 mm, and a standard deviation of 0.115. This shows that the empirical model derived from the designed experiment, was able to capture the behaviour of the dispensing process under the different levels of the studied parameters.

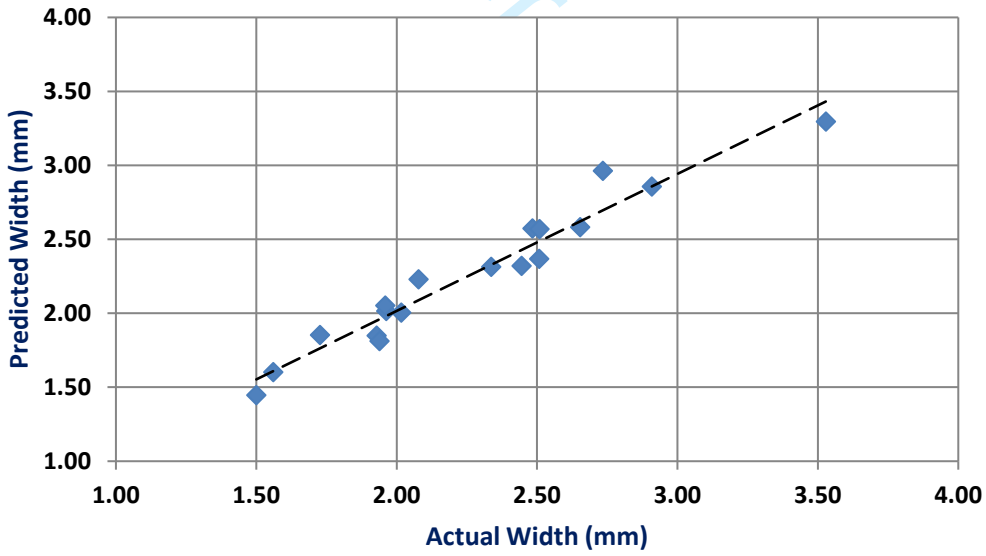

Figure 7: Predicted width values by the model vs. the actual values

Moreover, an important result from the design of experiment is the effect of each process parameters on the studied response. In order to better understand the behaviour of the process, the effect of varying the robot velocity on the resulting width of maskant lines under different values of pressure and needle diameter is plotted in Figure 8. Each point

on the graph represents the average width of the five maskant lines resulting from an individual experimental run. The graphs show that a change of width in the range of 0.5 mm is possible within the tested range of robot velocities (20 to 40 mm/s). The choice of needle diameter and applied pressure can clearly shift the range possible width values. Thus, the width of dispensed maskant lines can be controlled during the masking process through the robot velocity, while the range of feasible variation in the line width is determined by the selection of the pressure input and needle diameter at the beginning of the process.

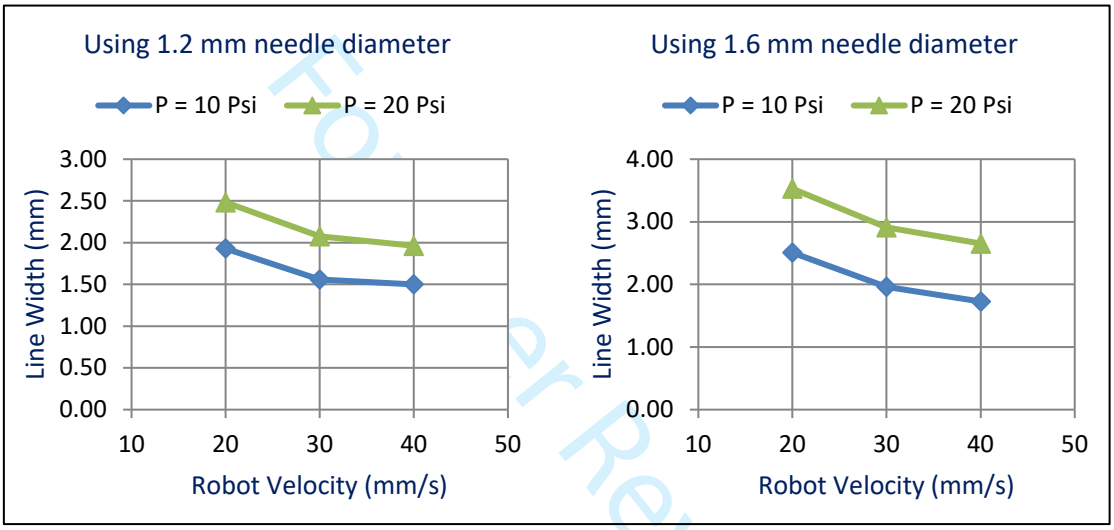

Figure 8: Effect of robot velocity on line width at different values of Pressure and Needle diameter

Samples of the dispensed masking lines in raster pattern with a different combination of factor levels are shown in Figure 9. This further illustrates that by varying the values of the investigated parameters, the width of the dispensed masking lines can be changed. However, care must be taken to avoid odd combinations of input values that might result in discontinued lines as shown in sample 12 in Figure 9. This resulted from excessively increasing the robot velocity relative to the fluid velocity leaving the needle. It is recommended to maintain the robot velocity to be less than or equal to the fluid velocity (can be approximated using Equation 6) at any instance during the dispensing process. Any further reduction required to the width of the dispensed lines should be achieved by initially selecting a finer needle diameter or smaller pressure value, rather than excessively increasing the robot velocity during operation.

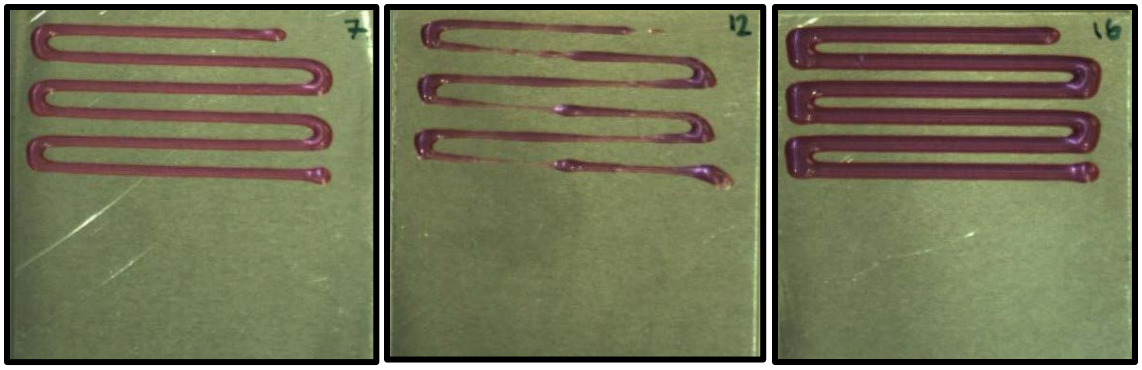

Figure 9: Samples of dispensed masking lines from the conducted experiment

As mentioned earlier, the modelling of the system has been simplified by ignoring the start and the end delay that occurs before a steady state condition is reached. This is demonstrated in the sample shown in Figure 10, in which the location of the start point is delayed by an offset distance, while the endpoint shows an accumulation of some excess material due to the delay in stopping the maskant flow. However, due to the nature of this application, the start and end delay can be practically overcome by starting and ending the masking at non-critical points. For example, when masking an area, the process can be started and ended inside the masked areas rather than at the edges. Hence, overcoming the effect of any variations in the width of dispensed lines at the start and end conditions by appropriate path planning. In addition, a simple weighting function can be used based on the experimental data to minimise the start/end delay issues as mentioned in section 3.1. This was implemented in the final experiment outlined in the next section.

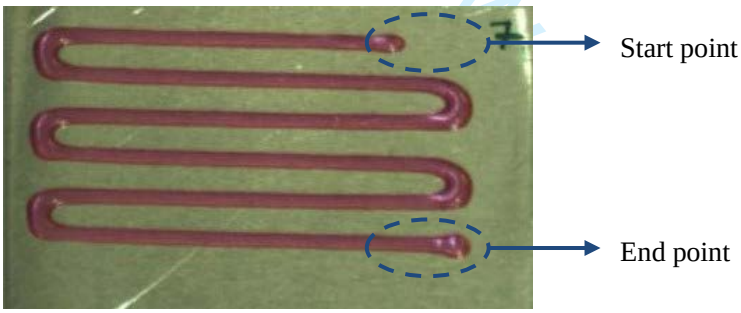

Figure 10: The effect of delay at the start and end points

3.2.2 Model Validation

In order to validation the empirical model, another experiment was conducted by feeding the model with new combinations of process parameter values and comparing the

measured width of dispensed lines to the values predicted by the derived empirical model. Table 2 summarises the values of the tested factors and the resulting maskant width measured using the imaging process, in comparison to the value predicted by the model. The results of the experiment showed that the model was still able to estimate the resulting masking line widths successfully with an average error of -0.3 mm and a standard deviation of only 0.06 mm. Figure 11 shows a plot comparison between the actual and predicted width values at the new tested input conditions.

Table 2: Experimental data from the verification tests

Run	Factors			Responses		
	VR	ΔP	Dn	Maskant Width (W)		
	mm/s	Psi	mm	predicted	actual	error
1	25	20	1.6	3.047	2.800	-0.247
2	35	20	1.6	2.706	2.347	-0.359
3	40	20	1.6	2.582	2.255	-0.327
4	30	20	1.6	2.857	2.545	-0.312
5	30	24	1.6	3.117	2.836	-0.281
6	30	26	1.6	3.239	2.848	-0.391
7	30	28	1.6	3.355	3.120	-0.235
				Average Error		-0.30
				Standard deviation		0.06

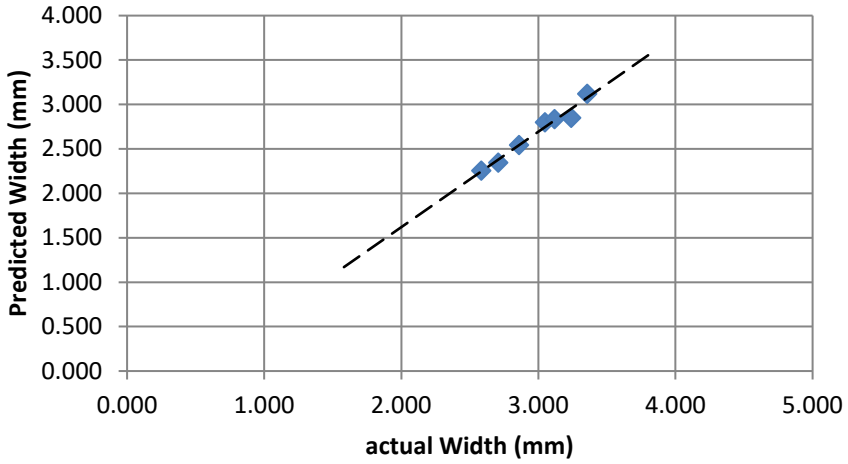

Figure 11: Comparing predicted to the actual width of masking lines as a Verification for the Empirical Model

The temperature was kept constant during the initial experiment to develop the empirical model and was again kept constant for the verification experiment. However, it has been noted that there was a room temperature difference of nearly 4.5ºC between the days of the development and verification experiments. This temperature difference is expected to be the cause of the systematic shift error witnessed in the results. Thus, insulating the syringe to limit the temperature variations alone is not sufficient, since room temperature may vary considerably on the long run causing a slight deviation from the width values predicted by the model. Hence, for applications requiring enhanced accuracy, it is recommended to also heat the syringe to a fixed known temperature, to ensure that the system will always be operating at the same exact temperature and yield consistent masking results.

4 Surface Masking Test

A final experiment was conducted with the aim of verification of the proposed automatic masking approach by masking a rectangular area on a flat surface. The derived model was used to decide on the proper combination of process parameters necessary to mask a rectangular area on a flat surface. A program was developed to automatically generate raster pattern paths for the robot arm based on the inputs parameters of (i) the starting point, (ii) number of maskant lines, (iii) line length, and (iv) the spacing between lines. Currently, the first three inputs are provided by the user based on the geometry of the

area to be masked, whilst the spacing parameter is automatically calculated based on the expected line width generated from the derived model. However, in the future, a path planning algorithm can aid in automating the first three inputs based on scanning the target area to be masked.

During this experiment, the robot arm was directed to place one corner of the rectangular test piece horizontally beneath the needle and record the coordinates of this point as the starting point. Knowing the dimensions of the test piece, the maskant line length was set to cover the length of the target plate, while the width of the plate and the desired number of lines in the raster pattern were fed to the controller to calculate the required line width and set the line spacing accordingly to achieve consistent area coverage. Since the number of lines must be an integer value and the width of each line can be varied as desired by adjusting the robot velocity, it made sense to supply the number of lines as a fixed input to the program and rely on the derived empirical model to calculate the robot velocity that would result in the desired line width for a given input pressure and needle diameter. An adjusted to the input pressure might be necessary if the resulting robot velocity is significantly larger than the maskant flow velocity. This might otherwise result in the dispensing of discontinuous lines as previously discussed. Hence, the value of the applied pressure and the needle diameter have to be set manually at the beginning of the operation based on the required range of masking widths, so that the range of robot velocities required throughout the masking operation would not result in any discontinuities.

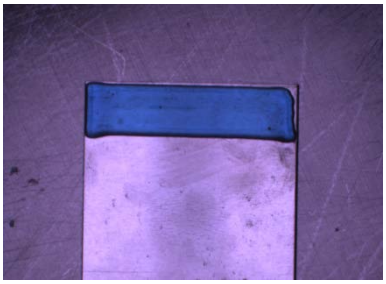

Figure 12: Masking a rectangular area on a flat plate

A sample test piece that was successfully masked is shown in Figure 12, which shows the result of masking an area of the plate following the raster pattern as described. An additional step to be implemented when more precise masking is required, would be to

apply a fine masking line accurately around the circumference of the area before filling the inside with thicker lines following a raster pattern. During the dispensing process, the robot velocity can be modified accurately with a fast response through the robot controller, to increase the width of dispensing lines when filling large areas and reduce it when masking accurately around the circumference of the masked area.

5 Conclusions and Future Work

In this paper, the T/P dispensing based masking process using a robotic manipulator has been modelled mathematically and empirically, in order to control the automated masking of areas with a consistent maskant layer. A mathematical model for the T/P dispensing process was derived, extending previous models from the literature by incorporating the robot velocity for controlled masking line width. The mathematical study laid the theoretical foundation for identifying the key parameters that affect the output of dispensing based masking process. An experimental study was designed accordingly to derive an empirical model from the generated data that incorporates the losses that are otherwise difficult to model mathematically. The final empirical model was experimentally validated by dispensing masking lines under new combinations of input parameters, measuring their actual width values using image processing, and comparing them to the values predicted by the model. The results showed a mean error of only -0.3 mm and a standard deviation of 0.06 mm, which confirms the perdition accuracy of the derived model for the tested operating range. In the final verification of the proposed approach, the proposed automated masking system was used to coat a planar area successfully with consistent coverage. This was achieved in a single stage as opposed to the current multi-stage manual masking, which is expected to reduce the overall masking time under similar conditions to around one-third of its current value (single masking and coating cycle rather than three).

The next stage of this work should involve masking of more complex objects, which will require investigating additional process parameters including: the needle angle, needle height, and robot velocity and acceleration. Additionally, the simplification of the masking process into steady-state one is only suitable for masking parts with simple

geometries. However, for more complex shapes, precise dynamic control will be required for masking around edges, sharp corners, and intricate features. This will enable dynamic compensation for the start/end delay according to the chosen process parameter. Furthermore, automatic path generation will be an essential improvement to the current system, in order to automatically decide the most efficient pattern for the robot to follow when filling the scanned target area.

Acknowledgements

The reported work has been partially funded by the EPSRC Centre for Innovated Manufacturing in Intelligent Automation (EP/IO33467/1). The support of which is gratefully acknowledged.

References:

1. O'Keefe M. Robotic Coatings Automation. *Technol Rev J* 2004; 22–33.
2. Destefani J. Custom Masking Helps Hixson Soar. (cover story). *Prod Finish* 2006; 70: 62–64.
3. Masking paints for airbus. *Aircr Eng Aerosp Technol* 2008; 80: aeat.2008.12780ead.028.
4. Jennerjohn PE. Unique Aspects Involved in the Robotic Painting of Commercial Aircraft Structures. In: *SAE Technical Paper*. SAE International. Epub ahead of print 2011. DOI: 10.4271/2011-01-2790.
5. Scafe AP. Developing robotic sealing processes in aerospace manufacturing. *SAE Technical Papers*; 6. Epub ahead of print 2012. DOI: 10.4271/2012-01-1854.
6. Fu Z, Zou L, Wu Y, et al. Automatic coating and fastening robot of space solar module to solar panel substrate. *Assem Autom* 2008; 28: 301–307.
7. Xie F, Liu X-J, Wu C, et al. A novel spray painting robotic device for the coating process in automotive industry. *Proc Inst Mech Eng Part C J Mech Eng Sci* 2015; 229: 2081–2093.
8. Pichler A, Bauer H, Eberst C, et al. Towards more Agility in Robot Painting

through 3D Object Recognition. *Intell Prod Mach Syst - 2nd I*PROMS Virtual Int Conf 3-14 July 2006* 2006; 608–613.

9. Kong F, Yuan L, Zheng YF, et al. Automatic liquid handling for life science: a critical review of the current state of the art. *J Lab Autom* 2012; 17: 169–85.

10. Mei Z, Maropoulos PG. Review of the application of flexible, measurement-assisted assembly technology in aircraft manufacturing. *Proc Inst Mech Eng Part B J Eng Manuf* 2014; 228: 1185–1197.

11. Jamshidi J, Kayani A, Iravani P, et al. Manufacturing and assembly automation by integrated metrology systems for aircraft wing fabrication. *Proc Inst Mech Eng Part B J Eng Manuf* 2010; 224: 25–36.

12. Becroft SA. Automated Painting for Aerospace, Challenges, Newer Technologies and Lessons Learned. *SAE Int J Aerosp* 2012; 5: 22–30.

13. Bin Ishak I, Fisher J, Larochelle P. Robot Arm Platform for Additive Manufacturing Using Multi-Plane Toolpaths. *Vol 5A 40th Mech Robot Conf* 2016; V05AT07A063.

14. Yilmaz O, Ugla AA. Shaped metal deposition technique in additive manufacturing: A review. *Proc Inst Mech Eng Part B J Eng Manuf* 2016; 230: 1781–1798.

15. Donghong Ding, Zengxi Pan, Dominic Cuiuri HL. A multi-bead overlapping model for robotic wire and arc additive manufacturing. *Robot Comput Integr Manuf*; 31.

16. Zhang GQ, Mondesir W, Martinez C, et al. Robotic additive manufacturing along curved surface - A step towards free-form fabrication. *2015 IEEE Int Conf Robot Biomimetics, IEEE-ROBIO 2015* 2015; 721–726.

17. Reighard M;, Barendt ANA. *Conformal Coating Process Controls: The Manufacturing Engineer's Aid*. 2000.

18. Li HX, Liu J, Chen CP, et al. A simple model-based approach for fluid dispensing analysis and control. *IEEE/ASME Trans Mechatronics* 2007; 12: 491–503.

19. Jianping L, Guiling D. Technology development and basic theory study of fluid dispensing - a review. *High Density Microsyst Des Packag Compon Fail Anal 2004 HDP '04 Proceeding Sixth IEEE CPMT Conf* 2004; 198–205.

20. Chen XB. Modeling and control of fluid dispensing processes: A state-of-the-art review. *Int J Adv Manuf Technol* 2009; 43: 276–286.

21. Liu Y, Chen L, Sun L. Automated precise liquid dispensing system a for protein crystallization. *Proc 2007 IEEE Int Conf Mechatronics Autom ICMA 2007* 2007; 3616–3621.

22. Chen RS, Sun CM. A collaborative continuous auditing model under service-oriented architecture environments. *Proc 6th Wseas Int Conf E-Activities* 2007; 45–50.

23. Zhao YX, Li HX, Ding H, et al. Integrated modelling of a time-pressure fluid dispensing system for electronics manufacturing. *Int J Adv Manuf Technol* 2005; 26: 1–9.

24. Chen CP, Li HX, Ding H. Modeling and control of time-pressure dispensing for semiconductor manufacturing. *Int J Autom Comput* 2007; 4: 422–427.

25. Jianping W, Huai Z, Xiulun L. Performance of a new vapor-liquid-solid three-phase circulating fluidized bed evaporator. *Chem Eng Process Process Intensif* 2004; 43: 49–56.

26. Lewis A, Babiarz A. Conductive Adhesive Dispensing Process Considerations.

27. Chen XB, Kai J. Modeling of positive-displacement fluid dispensing processes. *IEEE Trans Electron Packag Manuf* 2004; 27: 157–163.

28. Chen XB, Zhang WJ, Schoenau G, et al. Off-line control of time-pressure dispensing processes for electronics packaging. *IEEE Trans Electron Packag Manuf* 2003; 26: 286–293.

29. Zhao YX, Li HX, Ding H, et al. Integrated modelling of a time-pressure fluid dispensing system for electronics manufacturing. *Int J Adv Manuf Technol* 2005; 26: 1–9.